



Stabilising Large Grains in Aggrading Steep Channels

William H. Booker¹ and Brett C. Eaton¹

¹Geography Department, University of British Columbia, Vancouver, BC, Canada

Correspondence: William H. Booker (william.booker@alumni.ubc.ca)

Abstract. It is understood that the interaction between sediment supply and discharge drives first-order behaviour of deposits. The influence of the grain size distribution shape over the mobility and resultant evolution is, however, unclear. Four experiments were conducted in a scaled physical model for two grain size distributions, analogous to a one-dimensional self-formed alluvial fan. We demonstrate the unsuitability of the median grain size as a predictor of deposit behaviour at flows when the material is not equally mobile. The results instead suggest, during conditions of unequal mobility, that largest grains control the transport efficiency of the overall sediment mixture, and thus also the morphodynamics of the deposit and its tendency to store or evacuate material. Deposits appear to show a dependence upon the rate of material supply more strongly when the likelihood of its motion is less equally distributed (i.e., under partial transport conditions). If the coarse fraction (e.g., greater than 84th percentile) is instead mobile due to increased discharge or because of their relative size, transport rates will increase and the behaviour of the mixtures converge to a common state, with morphology influenced by the material's mobility.

1 Introduction

Gravel bed rivers adjust their boundaries from the grain to the reach scale in response to the supplied sediment and water discharges (Eaton and Church, 2004). The feedbacks and interactions between antecedent flow and sediment discharge control the river channel form (Fukuoka, 1989), and thereby influence channel response to new stimuli. Natural channels are likely to experience a distribution of flow rates and, therefore, corresponding modes of transport (e.g., Ashworth and Ferguson, 1989; Warburton, 1992). Central to the behaviour of gravel bed rivers is this proclivity for adjustment in response to their environment as the flow does not regularly or greatly exceed the threshold of sediment mobility (e.g., Church, 2006). Instead surficial adjustment, bed forms and macroforms modulate bed material sediment transport rate, acting to dissipate energy and provide stability to the overall channel (Cherkauer, 1973). For example, grains may stabilise through rotation (Masteller and Finnegan, 2017), their organisation into cells (Church et al., 1998) and the formation of alternate bars (Lisle et al., 1991).

One of the most well studied of these phenomena is the coarsening of the bed surface that results from the preferential removal of fine grains, until an armour layer develops that approximately equalises the threshold entrainment stress of the bed (Parker and Klingeman, 1982; Parker et al., 1982; Andrews, 1983). Armour may develop in both sediment-starved reaches, as static armour (e.g., Kondolf, 1997), or where sediment supply is present, as mobile armour (e.g., Andrews and Parker, 1987). It is the formation of an armour layer that prevents continued transport of the bed material and stabilises the channel against further deformative work. However, armour formation is inherently a degradational process that acts to limit the mobility of



the bed surface and is therefore suppressed in environments where material is being deposited. In general, aggrading gravel bed river systems are poorly studied, despite their frequent occurrence on alluvial fans and in mountainous environments with high sediment loads. Accordingly, our knowledge of the controls over stability in such environments is limited. These systems maintain sediment conveyance through the processes acting in opposition to those observed during degradation. Chiefly this has been observed as sediment mobility changes through bed organisation (Lisle et al., 1991) and slope changes to increase shear stress (Bryant et al., 1995). In contrast to degrading channels it appears as if there are fewer mechanisms acting to limit change to channel dimensions (i.e., confer stability).

In a channel the aggradation or degradation of material will lead to changes in its elevation, representing a balance between the amount of energy and material provided to it. Lane (1955) proposed that grade represents this balance as:

$$10 \quad \frac{Q_b}{QS} \propto \frac{1}{D} \quad (1)$$

wherein the left hand side of the proportionality represents the sediment transport efficiency, given by the ratio between sediment supply (Q_b) and the product of discharge (Q) and slope (S). The right hand side represents the calibre of the sediment flux (D), and is typically assumed to be the median size of the bed material (D_{50}). Accordingly, mixtures of the same median grain size, under the same water and sediment discharges, should form to the same slope given by their transport efficiency. Transport efficiency is used in the same manner as Bagnold (1966), in that it relates the work rate of the flow to the stream power available and describes the efficiency of the system in converting stream power into work (i.e., sediment transport) and is therefore higher in more efficient systems. Here, it is reformulated neglecting the mass flux term from its original form, instead replicating the volumetric consideration used by Eaton and Church (2011):

$$20 \quad \eta = \frac{Q_b}{QS} \quad (2)$$

whereby it functions as a relationship between the system's mass and energy inputs, outputs and processes.

However, recent work has demonstrated that it is the largest grains found in the bed material that control channel stability during degradation, and channel stability cannot be fundamentally linked to the median bed surface grain size (MacKenzie and Eaton, 2017). If this is the case, then the assumptions underlying the use of Eq. (1) in degrading settings are called into question. We hypothesise that, like degrading systems, the presence of the large grains will result in different transport regimes, as in MacKenzie and Eaton (2017), and thus different channel morphodynamics and depositional slope. The goal of this paper, therefore, is to test whether or not large grains influence channel stability in aggrading systems, wherein many of the processes thought to produce stabilisation in degrading systems are suppressed. To that end, we present the results of four pairs of experiments, paired by median grain size but differentiated by the shape of their distributions, for which Eq. (1) would predict similar behaviour. In most studies, slope responds through the superposition of change upon a pre-existing mass. Here, sediment may freely aggrade or degrade and thus slope acts instead as an emergent indicator of the system state, thus allowing its form to fully represent the suite of process acting upon it. The results described herein show that the grain size distribution used affects the resultant behaviour, and the differences between paired experiments are controlled by the experimental boundary conditions.

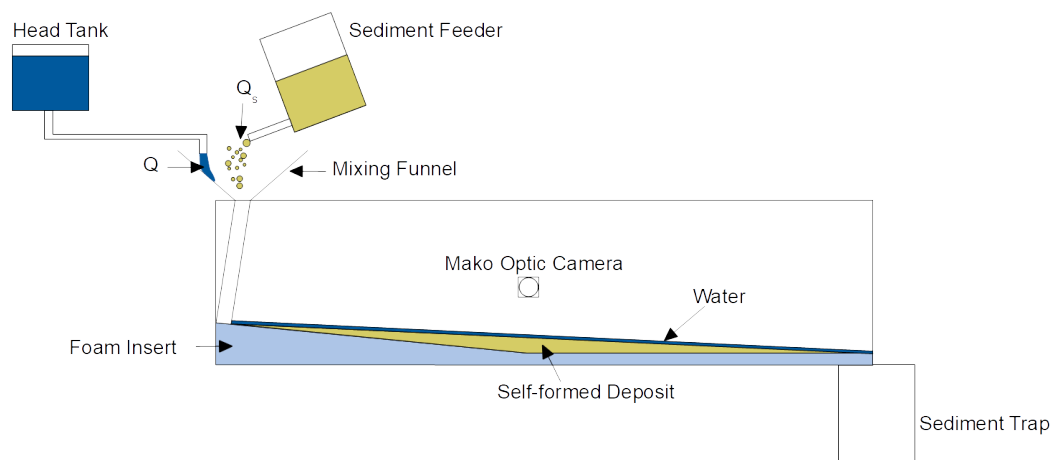


Figure 1. Simplified diagram of the experimental setup for the steep channel flume.

2 Methods

Eight experiments were run in the recently constructed steep mountain channel flume at the University of British Columbia. The flume is acrylic walled, 2 m long by 0.128 m wide with a foam insert creating a transition from a steep (slope = 0.1 m m^{-1}) upper and flat (slope = 0 m m^{-1}) lower section (Fig. 1), upon which a fan deposit can develop. These deposits that form within the flume are analogous to a one dimensional fan, or to the channel bed of a steep river confined by bedrock walls. Design and methodological cues were taken from previous experiments concerning self formed deposition (Guerit et al., 2014) and steep channel stability (Lisle et al., 1991).

During the runs reported herein, feed and flow were held constant for the length of the experiment. These were conducted under one of four conditions: 100L, 100H, 200L or 200H, where the number refers to the flow rate (in ml s^{-1}) and the letter feed rate ($L = 1 \text{ g s}^{-1}$, $H = 2 \text{ g s}^{-1}$). This range of values allows us to consider five relative changes in relative sediment concentration mediated by changes to discharge or sediment feed rate. Those are: no change in concentration but changes in the total flux magnitude (100L vs. 200H), doubling concentration through increasing sediment feed (100L vs. 100H), doubling concentration through decreasing discharge (200H vs. 100H), halving concentration through increasing discharge (100L vs. 200L) and halving concentration through sediment feed (200H vs. 200L). Similar to MacKenzie and Eaton (2017), the sediment is roughly scaled from gravel-bedded streams found in Alberta, Canada and truncated at 0.25 mm at the lower end to remove unscalable laminar sub-layer effects for sediment finer than this size limit (Peakall et al., 1996).

These eight experiments primarily serve to distinguish between the behaviour of two grain size distributions across a range of run conditions. The two grain size distributions share nearly the same D_{50} ($GSD_1 = 2.03 \text{ mm}$, $GSD_2 = 2.02 \text{ mm}$). The first grain size distribution (GSD_1) comprises a log-normal distribution from 0.25 mm to 8 mm (Fig. 2). The second distribution (GSD_2) is only comprised of two size classes; 1.4 to 2.0 mm and 2.0 to 2.8 mm (Fig. 2). As a result GSD_1 has a substantially higher D_{84} and standard deviation (σ), as would be expected from its substantially coarser and finer tails (Table 1).

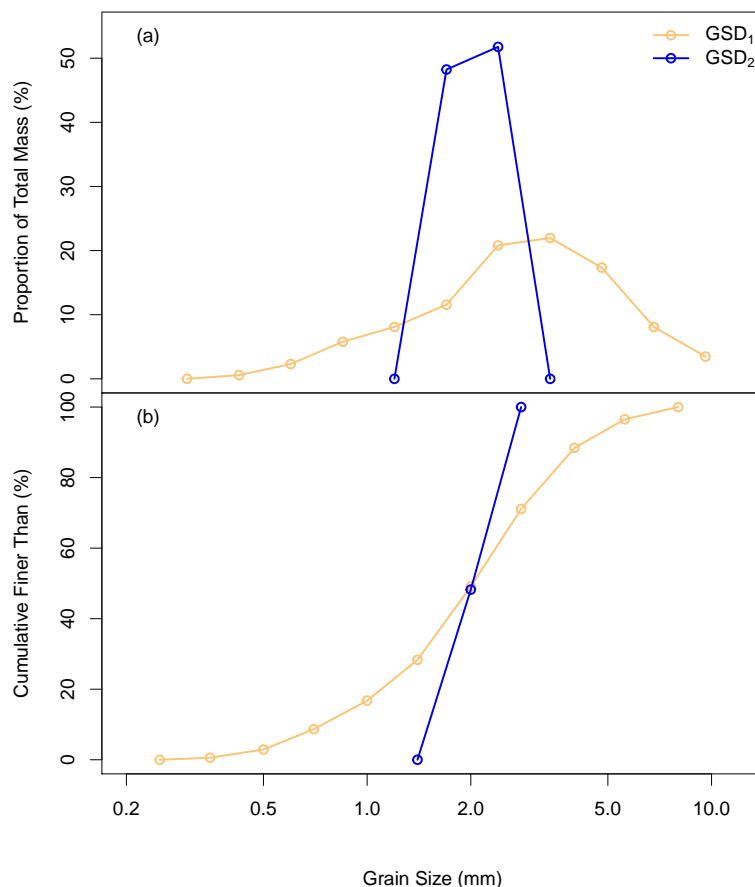


Figure 2. Grain size distributions for half-phi classes (a) individually and (b) cumulatively.

At the beginning of the experiment roughness elements were placed on the bed to ensure that the flow remained subcritical during the initial deposit building stages. Once the sediment feed and water supply were turned on, bed material deposited around the initial roughness elements, burying them and creating a freely adjustable self-formed deposit with a configuration dictated by the grain size distribution of the sediment supply. The data presented here is collected after sediment has begun to be output from the flume. That is, sediment has deposited along the length of the flume, and begun to be transported out and collecting in the sediment trap (see Fig. 3). By which time the channel has a self adjusted roughness and the influence of the roughness elements themselves is limited.

The main source of data used herein was collected using a side-looking camera to map the evolution of the channel's long profile. A Mako Optic camera was positioned perpendicular to flume orientation, and took photographs at 60 second intervals. The camera itself contains a routine to flatten these images and correct for radial lens distortion, resulting in a nearly perfect orthometric image. An image calibration routine translated pixel values to real space coordinates, from which a linear regression was fit to estimate the bulk sediment deposit gradient from the channel profile. Additionally, at 30 second intervals



Figure 3. Example image of roughness element sediment submergence taken during sediment output, from experiment G2Q100H.

oblique images of the bed were captured by a GoPro oriented upstream. The images were compiled into videos and submitted alongside this paper to record the bed state evolution (see Video availability).

Sediment output data was also recorded through the use of a sediment trap emptied at 15 minute intervals. The material captured, dried and then weighed, giving us mean transport rates for the preceding period and allowing us to calculate relative sediment storage efficiency, as the difference between output and input. Additionally, the mean transport rate is the value used in Eq. (2) in order to calculate η values reported later.

2.1 Slope Derivation

In order to derive a water surface slope from the profile images, a simple image classification process was applied to each frame. First a randomForests model was used to assign one of seven sub-classes to RGB pixel values built from a smoothed training image. The sub-classes within these are: sediment, clear water, water with sediment behind it (pool), water surface,

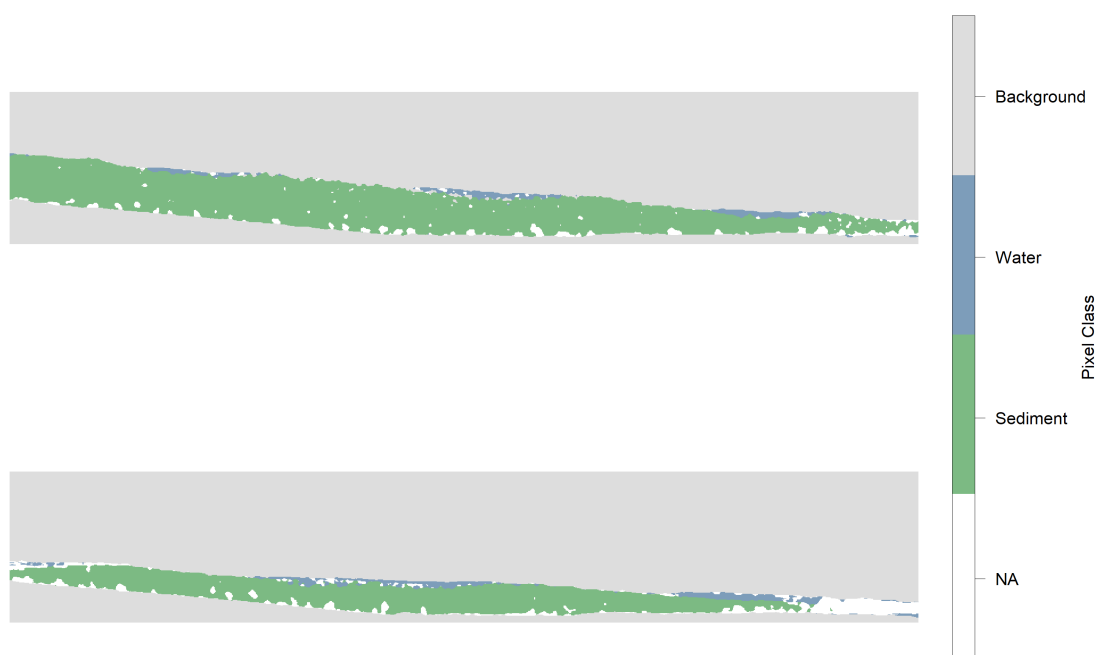


Figure 4. Output after image classification at end of aggradational phases for Exp. 100L using (a) GSD₁ (T = 327 min) and (b) GSD₂ (T = 150 min).

background, background with shadow and the roughness elements. These sub-classes were then grouped into four umbrella classes as sediment, water, background and roughness elements, with the latter treated as NA values, and then smoothed using a 7 x 7 mode pixel filter to reduce noise (Fig. 4). The slope values reported herein are the water surface slopes defined as the boundary between background class pixels and the highest of either water or sediment class pixels, until the downstream-most extent of sediment. As sediment may infill between the roughness elements but not contiguously deposit up to that point, a manual mask was applied to the height of the roughness elements to prevent the erroneous reporting of slope values.

3 Results

Panel (a) of Fig. 5 (relative sediment concentration = 1) shows a strong distinction between GSD₁ and GSD₂ for the full distribution of slopes, with the former organising to significantly higher values. Similarly, for twice the relative sediment concentration, a clear separation exists between the distributions of slopes formed by GSD₁ and GSD₂, albeit with a lower difference between the two. In contrast, at higher discharges the slopes for both sediment feed rates are distributed about a lower mean, and substantial overlap occurs between the lower bound of GSD₁ and the upper bound of GSD₂. The mean slope

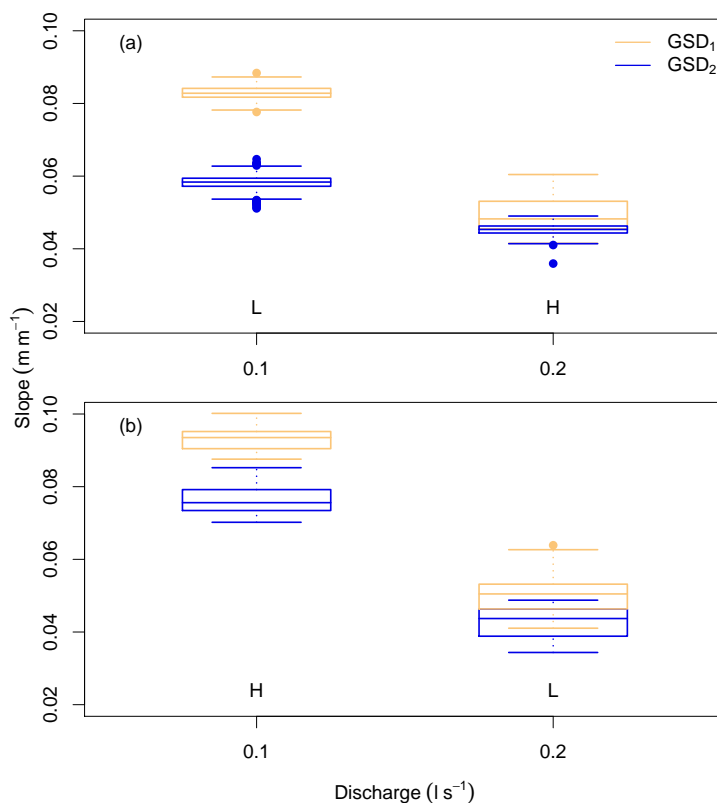


Figure 5. Distribution of slope values from the onset of transport onwards. Plots separate experiments by a) normal (i.e., 1) and b) not normal (i.e., 0.5 or 2) relative sediment concentration. Text indicates sediment feed rate (L = 1 g s⁻¹, H = 2 g s⁻¹).

value decreases for both grain mixtures at higher discharges, although it decreases more sharply for GSD₁. The raw values for which are shown in Table 2, and differences resulting from changes between run conditions are shown in Table 3.

Sediment output rates are shown in Table 4, and they show an increase in sediment transport efficiency in response to changes in discharge. For both grain sizes more material is stored at lower discharges correlating to the steeper angles of the deposits. Doubling the feed rate results in both systems retaining a higher proportion of sediment within the system at 100 ml s⁻¹. However when discharge is increased, regardless of feed rate, the two systems behave more similarly both with respect to feed rate and with each other.

Three key observations can be made regarding the distribution of transport efficiencies (Fig. 6). First, the efficiencies of GSD₁ are consistently lower than those of GSD₂ (Table 5), following from the differences in slope reported above. Second, increasing water discharge, for a given feed rate, increases the efficiency of both grain size distributions under both feed scenarios except for GSD₂ under low feed, where a decrease is observed (Table 6). Third, increasing feed rate, for a given

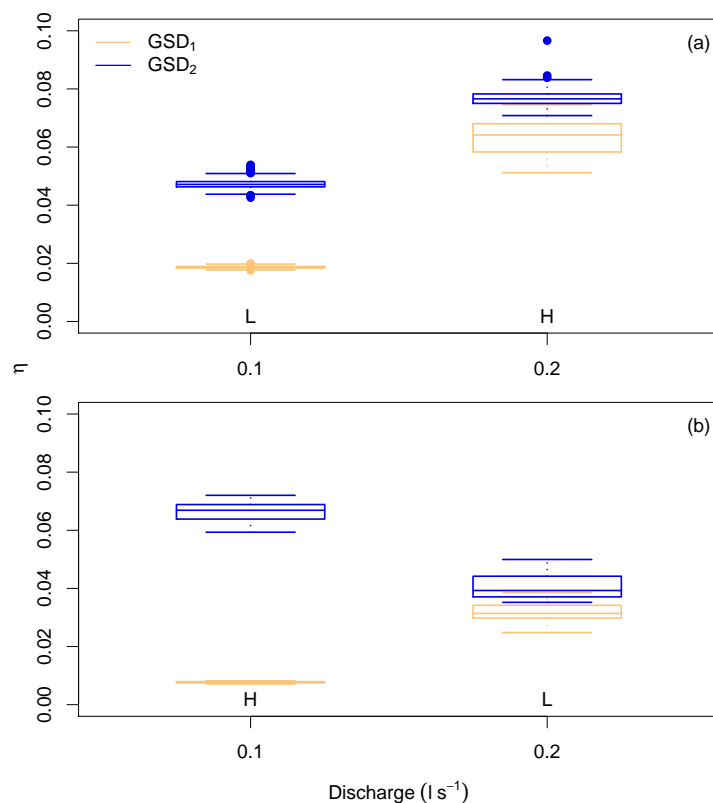


Figure 6. Distribution of transport efficiencies (η from Eq. (2)) for experiments 100L, 100H, 200L and 200H.

discharge, increases the efficiency of both grain size distributions except for GSD₁ with low discharge, where a decrease is observed (Table 6).

4 Discussion

The results of these experiments clearly demonstrate that the range of grain sizes present in the bed material, and load, exerts first-order control over self-formed deposition, is therefore inappropriate to simply use the median surface grain size in order to characterise the system under all conditions. The extent of this influence does, however, vary with the boundary conditions under which the experiments are conducted. At lower discharges, differences between the two grain size distributions can be attributed to the relative difficulty of the channel to mobilise the larger grains. Thus it is the volume of supplied material that influences the efficiency of transport.



The difference varying alongside discharge is shown by our primary response variable, slope. If we were to predict behaviour of the systems from the Lane relation (Eq. (1)), we would assume that both grain size distributions would behave in the same manner. Additionally, those experiments of the same sediment concentration (100L and 200H) would have the same values of slope. Further, where sediment concentration was increased or decreased, we would expect commensurate increases or decreases in slope respectively. However, one set of systems (i.e., those of the poorly sorted GSD_1) consistently organise to higher slopes and lower transport efficiencies than those for the more narrowly graded (i.e., GSD_2) systems for each experimental condition. As all systems were continuously accumulating, sediment surface armouring could not occur due to the suppression of selective transport and subsequent equivalence between the bed surface and sediment feed grain size distributions. Therefore, the observed differences in slope cannot be attributed to differing degrees of surface armouring. Instead, it is more likely due to bed surface sorting.

The strongly differing depositional slopes occurring at low discharges are at odds with what we know about sediment entrainment. Previous studies suggest that most of the bed material becomes entrained at about the same shear stress due to the relative hiding and exposure of grains smaller and larger than the median surface size (Parker et al., 1982; Parker and Klingeman, 1982). In addition, previous work indicates that the entrainment threshold for a unimodal mixture is similar to the entrainment threshold for a bed surface having the same median size (Komar, 1987). If we therefore extend this concept to the prediction of sediment deposition angles, then the existing body of work seems to suggest that the angles for our two grain size distributions ought to be effectively the same under the same boundary conditions.

A potentially critical explanation for this disparity is that equal mobility does not apply to all of the bed sediment. For example, Andrews (1983) found equal mobility applied only to sediment finer than about the bed surface D_{84} in his field study, and nearly all of the data on bed mobility published by Haschenburger and Wilcock (2003) showed similar relative stability of the largest grains at even the highest shear stresses. We believe this suggests that the size of the largest sediment in the bed may determine the deposition threshold for a mixture, at least for those situations in which competence controls sediment deposition, not sediment transport capacity. The implication of this position is that the gradient of fans, floodplains and other self-forming alluvial deposits is likely to be related to the size of the largest sediment in transport, not the median bed surface size as previously assumed.

Interestingly, there is also a marked difference in the efficiency of the two systems with respect to sediment transport (Fig. 6). For GSD_1 , the characteristic efficiency was substantially lower than it was for GSD_2 . This is at odds with the concept of channel grade proposed by Lane (1955), at least in its commonly used form (Eqn. (1)). Church (2006) recast this relation in a dimensionally balanced version, which can be written as follows:

$$\frac{Q_b}{QS} \propto \frac{d}{D} \quad (3)$$

In Church's version, D is specifically defined to be the median bed surface size, based on the understanding of the hiding/exposure processes controlling the entrainment of sediment from a mixture. Therefore, metrics derived from this relation, such as the transport efficiency consideration from Eaton and Church (2011), implicitly include this assumption and suffer the same limitation.



According to the conventions established by Lane (1955) and Church (2006), both of our grain size distributions had the same sediment calibre, so why did they not equilibrate at the same slope, and achieve the same transport efficiency? The average size of the sediment feed calibre is almost identical for both GSD_1 and GSD_2 . While we can explain the failure of Eq. (1) as stemming from its original intention to be used as a qualitative guide for thinking about channel grade, Eq. (3) is based on the existing semi-empirical representations of bed sediment entrainment, so the discrepancy between Eq. (3) and the results in Fig. 6 point to a more fundamental problem. Simply put, these results clearly indicate that D_{50} is a poor choice for the characteristic grain size, at least when considering the processes forming alluvial deposits at lower discharges (i.e., the majority of the time), rather than those eroding them or at least responsible for high rates of bedload transport. Our preliminary analysis suggests that some representation of the coarse tail is probably more appropriate (such as the D_{84} , which is commonly used in flow resistance equations).

At a basic level, the observed differences in slopes are associated with the varying ability of two experimental systems to transport sediment, which in turn is related to the relative thresholds of motion of the largest grains. Curran and Wilcock (2005) observed increased transport rates of coarse sediment at lower slopes, for the same discharge and coarse feed rate, as sand supply increased in their flume experiments. The same inference can be made here: deposits organise to a lower slope for GSD_2 because the sediment is more mobile. However, unlike the experiments by Curran and Wilcock (2005) the increased mobility is not due to the increased sand presence but the absence of the large immobile grains (e.g., MacKenzie and Eaton, 2017).

The idea that the stable slope angle for these experiments is determined by the mobility of the largest grains in the bed is consistent with existing equations predicting entrainment thresholds based on relative grain size. The reference stress (τ_r) required to mobilise a grain size fraction (i) is calculable using the approach published by Wilcock and Crowe (2003):

$$\frac{\tau_{ri}}{\tau_{rs50}} = \left(\frac{D_i}{D_{s50}} \right)^b \quad (4)$$

where τ_{rs50} is the reference stress for the median surface grain size and b is an exponent of value 0.67 when i is larger than the mean surface grain size. Equation (4) produces a shear stress 44.4% greater for entrainment of the D_{84} than the entrainment of the median in GSD_1 than in GSD_2 . This difference in mean slope values is approached during experiment 100L (GSD_1 is 42.7% higher than GSD_2), but is otherwise much higher than the observed differences in slope for the other experiments.

The decreasing difference in slope values as discharge increases indicates a cessation in the influence of the D_{84} and grain scale processes in driving larger scale behaviour. That is, the 8.88% difference in mean slope for 200H indicates that the mobility of the two mixtures are more similar and the role of the previously individual stabilising grains are reduced, minimising the differences between the two mixtures. Whilst the behaviours of the two mixtures never fully converge, the differences at low discharges and similarities at high discharges do suggest the presence of a threshold evident through these experiments that, once exceeded, causes the mobilities of the two mixtures to approach parity.

This suggestion of behaviour is similar to the observations of partial and full mobility under differing flow strengths by Wilcock and McArdell (1993). This separation between transport regimes at low and high discharges is also similar to the observation of the three phase transport model of Ashworth and Ferguson (1989), where equal mobility is achieved above a



threshold discharge. However, unlike Ashworth and Ferguson (1989), the increased transport rates are not generated through the destruction of previously organised structures, which necessarily require a range of flows without transport to form. Instead, the difference is sourced from an increase in the maximum grain size entrainable by the flow, and the likelihood of that grain's entrainment. That we see a poorly sorted mixture (GSD_1) acting in a manner similar to one that is well sorted (GSD_2) at higher discharges suggests that Eq. (3) is applicable when there is equal sediment mobility.

Pfeiffer et al. (2017) proposed that sediment supply controls the channel's hydraulic geometry, as well as the surface size of the material. This seems to be the case where the limit over transport is competence driven (i.e., flow = L) and thus the addition of greater volumes of sediment will force higher slopes, which is then reflected in the η values. However, when the systems have a higher likelihood and frequency of entraining the material at higher flows, the effects of sediment supply change are taken up by greatly increased sediment transport efficiency and minimal physical slope changes. The likelihood that this distinction would hold in natural streams is contentious, given the greater degree of confinement present using this setup than would be present in most fully alluvial settings; such a degree of confinement would likely only be found where streams are in close proximity to the valley walls. It is the concentration of flow enabled by the flume that allows high shear values to arise, without which the stream would laterally adjust by widening. This will therefore limit the ability to form deposits at a state where competence limit is not present, meaning natural systems are more likely to behave as the low discharge cases observed herein.

The differences in morphodynamics extend beyond reach average, 1D parameters like depositional slope and transport efficiency. Our observations of the bed dynamics has highlighted the important role that surficial organisation plays in controlling channel morphology and influencing sediment transport rates. Even the relatively narrow flume that we used (i.e $W = 0.128$ m) enabled the formation of secondary resistance elements such as bars.

The alternate bar morphodynamics we observed during some runs are not unprecedented; Lisle et al. (1991) reported similar morphodynamics, albeit with a lower slope than these experiments (Table 7). Lisle et al. (1991) also observed the formation of stationary (non-migrating) lateral bars with the bed surface separated into congested and smooth zones for an experiment having a similar grain size distribution.

Bed forms can influence sediment transport efficiency through the dissipation of energy and increased channel stability (Cherkauer, 1973; Hey, 1988; Prancevic and Lamb, 2015), and the bar characteristics are strongly linked to the maximum size of sediment in the bed material. In GSD_1 , bars were more persistent in time and space than in GSD_2 due to the importance of large grains as stabilising features for bars. In the case of GSD_1 , the largest grains clearly deposited first, creating a locus of deposition around which the bar head formed, allowing additional sediment to accumulate in its wake. The bars formed during GSD_2 were comprised of virtually the same size sediment, which can be entrained over a narrow range of shear stresses. As a result, the whole bar may be entrained at a similar shear stress, making these features more transient, and reducing their overall effect on bed stability. It is important to note that the stabilisation of the large grains in our experiment using GSD_1 was not the result of jamming, as described by Church (2006). The size of our flume was such that the ratio of the flume width to D_{84} was greater than 6, which is the jamming ratio proposed by Zimmermann et al. (2010).



The formation of lateral bars allows the transport of bed load through the contraction of the channel width increasing unit stream power as flow is concentrated (Lisle, 1987). This organisation of the bed surface into zones of transport and deposition thus maximises the efficiency of the channel and enables the previously limited transmittance of sediment and the growth of the depositional lobe. The wavelengths of the barforms we observed in higher sediment output experiments are longer than those of high sediment storage. Pyrcce and Ashmore (2005) demonstrated that the wavelength of bar spacing is a function of the transport lengths of bed load particles at channel forming flows; material is more mobile in higher wavelength reaches. Transport length is the distance between entrainment (τ_{ce}) and distraintment (τ_{cd}), therefore it is dependent on when the grain is deposited. Ancey et al. (2002) observed a type of hysteretic difference between these two thresholds, where the specific flow rate (and thus stress) necessary to induce deposition is lower than the entraining flow. Given the differences in entraining threshold between the mixtures it follows that the distrainting threshold for GSD₁ will be higher than for GSD₂, such that a smaller decrease is needed to trigger deposition. Therefore the systems can be characterised by the difference in behaviour of the coarse grains comprising the bar head loci (Pyrcce and Ashmore, 2005). For the more equally mobile GSD₂ this is manifested in a decreased likelihood of deposition of these grains, triggering longer path lengths and greater bar wavelengths in the system. In other words, the likelihood of entrainment ($P[\tau > \tau_{ce}]$) is greater in GSD₂, setting a lower overall deposit slope, whereas the likelihood of distraintment ($P[\tau < \tau_{cd}]$) is higher in GSD₁, decreasing transport length. This difference in reduced as discharge increases because the likelihood of entrainment increases, and distraintment decreases, for both mixtures but more strongly for GSD₁.

We can therefore consider the systems generated by GSD₂ as less stable on three accounts. Firstly, they developed at lower slopes and, as a result, were able to prograde more quickly due to reduced deposit volume. Secondly, the grains were more equally mobile due to a lower maximum threshold stress (i.e., smaller coarse fraction). Thirdly, the degree of surficial organisation was lower and bedforms were less persistent. The combination of these factors results in a system that does not need to concentrate flow in order to exceed threshold stress, despite the flow's lower slope and stream power, indicating its ability to transport sediment more efficiently than in experiments using GSD₁.

5 Conclusions

The eight experiments presented here demonstrate a difference in the self-adjusted slope and morphodynamics of aggrading systems derived from the difference of their grain size distributions and mediated by the relative sediment concentration. According to the prevailing theory that the median grain size is predictive of channel behaviour, the systems described within this paper should have exhibited similar slopes and patterns of morphodynamics under the same boundary conditions. Instead, the deposit formed from the more widely distributed GSD₁ developed to a higher slope, with lower transport efficiency, and demonstrated a greater degree of surface organisation. We argue that this is the result of the large grains in GSD₁ that exceed the competence of the flow, and require channel narrowing in order to mobilise. Where these grains are absent (i.e., GSD₂) the channel fails to achieve the highest state of organisation (i.e., lateral bars with narrow thalweg) as regularly because of the equally mobile sediment and bars. This difference decreases as you increase the discharge (i.e., entraining stresses) Thus



channel stability is linked not to the mobility of the median grain size, but to the mobility of the largest grains (e.g., D_{84}). We therefore conclude that the difference in behaviour between these systems is driven by a competence limitation of the larger grains. These findings indicate that models including sediment transport and conceptualising stability, such as regime models, need to consider the characteristic grain size as a coarser fraction than the median in order to more realistically replicate

5 behaviour in aggrading systems.

Code and data availability. Both the code and data used to create Figures 2, 4, 5 and 6 are available online (<http://doi.org/10.5281/zenodo.2672918>).

Video supplement. Videos of the bed morphodynamics are available online; GSD₁: Q100L (<http://doi.org/10.5446/41771>), Q200H (<http://doi.org/10.5446/41772>), Q100H (<http://doi.org/10.5446/41773>), Q200L (<http://doi.org/10.5446/41774>), GSD₂: Q100L (<http://doi.org/10.5446/41775>), Q200H (<http://doi.org/10.5446/41776>), Q100H (<http://doi.org/10.5446/41778>),

10 Q200L (<http://doi.org/10.5446/41777>).

Author contributions. W.H. Booker collected and analysed the data used in the paper, drafted the manuscript, and created the figures and tables; B.C. Eaton organised, reviewed and edited the manuscript.

Competing interests. The authors declare that they have no conflict of interest.



References

- Ancey, C., Bigillon, F., Frey, P., Lanier, J., and Ducret, R.: Saltating Motion of a Bead in a Rapid Water Stream, *Physical Review E*, 66, 036306, <https://doi.org/10.1103/PhysRevE.66.036306>, 2002.
- Andrews, E. D.: Entrainment of Gravel from Naturally Sorted Riverbed Material, *Geological Society of America Bulletin*, 94, 1225–1231, [https://doi.org/10.1130/0016-7606\(1983\)94<1225:EOGFNS>2.0.CO;2](https://doi.org/10.1130/0016-7606(1983)94<1225:EOGFNS>2.0.CO;2), 1983.
- Andrews, E. D. and Parker, G.: Formation of a Coarse Surface Layer as the Response to Gravel Mobility., in: *Sediment Transport in Gravel-Bed Rivers*, edited by Thorne, C., Bathurst, J., and Hey, pp. 269–300, Wiley, New York, 1987.
- Ashworth, P. J. and Ferguson, R. I.: Size-Selective Entrainment of Bed Load in Gravel Bed Streams, *Water Resources Research*, 25, 627–634, <https://doi.org/10.1029/WR025i004p00627>, 1989.
- 10 Bagnold, R. A.: *An Approach to the Sediment Transport Problem from General Physics*, U.S. Government Printing Office, 1966.
- Bryant, M., Falk, P., and Paola, C.: Experimental Study of Avulsion Frequency and Rate of Deposition, *Geology*, 23, 365–368, [https://doi.org/10.1130/0091-7613\(1995\)023<0365:ESOAFA>2.3.CO;2](https://doi.org/10.1130/0091-7613(1995)023<0365:ESOAFA>2.3.CO;2), 1995.
- Cherkauer, D. S.: Minimization of Power Expenditure in a Riffle-Pool Alluvial Channel, *Water Resources Research*, 9, 1613–1628, <https://doi.org/10.1029/WR009i006p01613>, 1973.
- 15 Church, M.: Bed Material Transport and the Morphology of Alluvial River Channels, *Annual Review of Earth and Planetary Sciences*, 34, 325–354, <https://doi.org/10.1146/annurev.earth.33.092203.122721>, 2006.
- Church, M., Hassan, M. A., and Wolcott, J. F.: Stabilizing Self-Organized Structures in Gravel-Bed Stream Channels: Field and Experimental Observations, *Water Resources Research*, 34, 3169–3179, <https://doi.org/10.1029/98WR00484>, 1998.
- Curran, J. and Wilcock, P. R.: Effect of Sand Supply on Transport Rates in a Gravel-Bed Channel, *Journal of Hydraulic Engineering*, 131, 961–967, 2005.
- 20 Eaton, B. C. and Church, M.: A Graded Stream Response Relation for Bed Load–Dominated Streams, *Journal of Geophysical Research: Earth Surface*, 109, F03011, <https://doi.org/10.1029/2003JF000062>, 2004.
- Eaton, B. C. and Church, M.: A Rational Sediment Transport Scaling Relation Based on Dimensionless Stream Power, *Earth Surface Processes and Landforms*, 36, 901–910, <https://doi.org/10.1002/esp.2120>, 2011.
- 25 Fukuoka, S.: Finite Amplitude Development of Alternate Bars, in: *River Meandering*, edited by Ikeda, S. and Parker, G., pp. 237–265, American Geophysical Union, <https://doi.org/10.1029/WM012p0237>, 1989.
- Guerit, L., Métivier, F., Devauchelle, O., Lajeunesse, E., and Barrier, L.: Laboratory Alluvial Fans in One Dimension, *Physical Review E*, 90, 022203, <https://doi.org/10.1103/PhysRevE.90.022203>, 2014.
- Haschenburger, J. K. and Wilcock, P. R.: Partial Transport in a Natural Gravel Bed Channel, *Water Resources Research*, 39, 1020, <https://doi.org/10.1029/2002WR001532>, 2003.
- 30 Hey, R.: Bar Form Resistance in Gravel-Bed Rivers, *Journal of Hydraulic Engineering*, 114, 1498–1508, [https://doi.org/https://doi.org/10.1061/\(ASCE\)0733-9429\(1988\)114:12\(1498\)](https://doi.org/https://doi.org/10.1061/(ASCE)0733-9429(1988)114:12(1498)), 1988.
- Komar, P. D.: Selective Grain Entrainment by a Current from a Bed of Mixed Sizes; a Reanalysis, *Journal of Sedimentary Research*, 57, 203–211, <https://doi.org/10.1306/212F8AE4-2B24-11D7-8648000102C1865D>, 1987.
- 35 Kondolf, G. M.: PROFILE: Hungry Water: Effects of Dams and Gravel Mining on River Channels, *Environmental Management*, 21, 533–551, <https://doi.org/10.1007/s002679900048>, 1997.



- Lane, E. W.: The Importance of Fluvial Morphology in Hydraulic Engineering, *Proceedings of the American Society of Civil Engineers*, 81, 1–17, 1955.
- Lisle, T. E.: Overview: Channel Morphology and Sediment Transport in Steepland Streams, In: R. Beschta, T. Blinn, G. E. Grant, F. J. Swanson, and G. G. Ice (ed.), *Erosion and Sedimentation in the Pacific Rim (Proceedings of the Corvallis Symposium, August 1987)*.
5 International Association of Hydrological Sciences Pub. No. 165, p. 287-297., 1987.
- Lisle, T. E., Ikeda, H., and Iseya, F.: Formation of Stationary Alternate Bars in a Steep Channel with Mixed-Size Sediment: A Flume Experiment, *Earth Surface Processes and Landforms*, 16, 463–469, <https://doi.org/10.1002/esp.3290160507>, 1991.
- MacKenzie, L. G. and Eaton, B. C.: Large Grains Matter: Contrasting Bed Stability and Morphodynamics during Two Nearly Identical Experiments, *Earth Surface Processes and Landforms*, 42, 1287–1295, <https://doi.org/10.1002/esp.4122>, 2017.
- 10 Masteller, C. C. and Finnegan, N. J.: Interplay between Grain Protrusion and Sediment Entrainment in an Experimental Flume, *Journal of Geophysical Research: Earth Surface*, 122, 274–289, <https://doi.org/10.1002/2016JF003943>, 2017.
- Parker, G. and Klingeman, P. C.: On Why Gravel Bed Streams Are Paved, *Water Resources Research*, 18, 1409–1423, <https://doi.org/10.1029/WR018i005p01409>, 1982.
- Parker, G., Klingeman, P. C., and McLean, D. G.: Bedload and size distribution in paved gravel-bed streams, *Journal of the Hydraulics
15 Division - ASCE*, 108, 544–571, 1982.
- Peakall, J., Ashworth, P., and Best, J.: Physical Modelling in Fluvial Geomorphology: Principles, Applications and Unresolved Issues, in: *The Scientific Nature of Geomorphology*, edited by Rhoads, B. L. and Thorn, C., pp. 221–253, John Wiley & Sons, Ltd, Chichester, 1996.
- Pfeiffer, A. M., Finnegan, N. J., and Willenbring, J. K.: Sediment Supply Controls Equilibrium Channel Geometry in Gravel Rivers, *Proceedings of the National Academy of Sciences*, 114, 3346–3351, <https://doi.org/10.1073/pnas.1612907114>, 2017.
- 20 Prancevic, J. P. and Lamb, M. P.: Unraveling Bed Slope from Relative Roughness in Initial Sediment Motion, *Journal of Geophysical Research: Earth Surface*, 120, 2014JF003 323, <https://doi.org/10.1002/2014JF003323>, 2015.
- Pyrce, R. S. and Ashmore, P. E.: Bedload Path Length and Point Bar Development in Gravel-Bed River Models, *Sedimentology*, 52, 839–857, <https://doi.org/10.1111/j.1365-3091.2005.00714.x>, 2005.
- Warburton, J.: Observations of Bed Load Transport and Channel Bed Changes in a Proglacial Mountain Stream, *Arctic and Alpine Research*,
25 24, 195–203, <https://doi.org/10.2307/1551657>, 1992.
- Wilcock, P. R. and Crowe, J. C.: Surface-Based Transport Model for Mixed-Size Sediment, *Journal of Hydraulic Engineering*, 129, 120–128, [https://doi.org/10.1061/\(ASCE\)0733-9429\(2003\)129:2\(120\)](https://doi.org/10.1061/(ASCE)0733-9429(2003)129:2(120)), 2003.
- Wilcock, P. R. and McArdell, B. W.: Surface-Based Fractional Transport Rates: Mobilization Thresholds and Partial Transport of a Sand-Gravel Sediment, *Water Resources Research*, 29, 1297–1312, <https://doi.org/10.1029/92WR02748>, 1993.
- 30 Zimmermann, A., Church, M., and Hassan, M. A.: Step-Pool Stability: Testing the Jammed State Hypothesis, *Journal of Geophysical Research: Earth Surface*, 115, F02 008, <https://doi.org/10.1029/2009JF001365>, 2010.



Table 1. Grain size metrics of the two distributions.

	D ₅₀	D ₈₄	σ
GSD ₁	2.03	3.65	1.38
GSD ₂	2.02	2.52	0.43

Table 2. Mean slope values and standard deviations, for the eight experiments reported here.

	GSD ₁		GSD ₂	
	Mean	St. Dev.	Mean	St. Dev.
100L	8.29×10^{-2}	1.96×10^{-3}	5.81×10^{-2}	2.21×10^{-3}
100H	9.30×10^{-2}	2.99×10^{-3}	7.68×10^{-2}	3.93×10^{-3}
200L	4.98×10^{-2}	4.28×10^{-3}	4.28×10^{-2}	3.89×10^{-3}
200H	4.92×10^{-2}	4.36×10^{-3}	4.52×10^{-2}	1.57×10^{-3}

Table 3. Changes in mean slope for the column name experiment, given relative to the row name experiment, for GSD₁ and GSD₂ respectively. Values are given in percent.

	100L	100H	200L	200H
100L	-	12.2/32.1	-40.0/-26.4	-40.6/-22.2
100H	-10.9/-24.3	-	-47.1/-41.1	-46.5/-44.3
200L	66.7/35.9	86.9/79.6	-	-1.03/5.77
200H	68.4/28.5	88.9/69.8	1.05/-5.46	-



Table 4. Output of sediment during each experiment, from the time sediment output occurred. The proportion of sediment output is relative to the volume input over the same timespan.

	Mean Output Rate (g s^{-1})		Proportion During Output (%)	
	GSD ₁	GSD ₂	GSD ₁	GSD ₂
100L	0.41	0.73	40.7	72.9
100H	0.19	1.34	8.5	66.4
200L	0.84	0.91	83.7	90.6
200H	1.64	1.84	81.7	91.4

Table 5. Mean transport efficiencies and their standard deviation.

	GSD ₁		GSD ₂	
	Mean	St. Dev.	Mean	St. Dev.
100L	1.87×10^{-2}	4.42×10^{-4}	4.75×10^{-2}	2.21×10^{-3}
100H	3.21×10^{-2}	2.81×10^{-3}	4.05×10^{-2}	3.82×10^{-3}
200L	7.71×10^{-3}	2.48×10^{-4}	6.60×10^{-2}	3.29×10^{-3}
200H	6.33×10^{-2}	5.50×10^{-3}	7.68×10^{-2}	2.80×10^{-3}

Table 6. Changes in mean transport efficiency for the column name experiment, given relative to the row name experiment, for GSD₁ and GSD₂ respectively. Values are given in percent.

	100L	100H	200L	200H
100L	-	-58.7/39.1	71.9/-14.7	239/61.9
100H	142/-28.1	-	316/-38.6	721/16.4
200L	-41.8/17.2	-76.0/63.0	-	97.3/89.8
200H	-70.5/-38.2	-87.8/-14.1	-49.3/-47.3	-

Table 7. Flume dimensions and run conditions for Lisle et al. (1991) and the two 100L experiments included here.

	Lisle et al. (1991)	G1Q100L	G2Q100L
Length (m)	7.5	2	2
Width (m)	0.3	0.128	0.128
Slope (m/m)	0.03	0.068	0.092
Grain Size Range (mm)	0.35-8	0.25-8.0	1.4-2.8
D ₅₀ (mm)	1.4	2.02	2.03
Flow Rate (ml s^{-1})	582	100	100
Feed Rate (g s^{-1})	8.4	1	1
Run Time (min)	560	549	429